Appl Phys B (2010) 98: 751–757
DOI 10.1007/s00340-009-3802-7

Applied Physics B
Lasers and Optics

Quasi-monolithic ring resonator for efficient frequency doubling of an external cavity diode laser

D. Skoczowsky · A. Jechow · H. Stürmer · T. Poßner · J. Sacher · R. Menzel

Received: 13 July 2009 / Revised version: 5 October 2009 / Published online: 1 November 2009

Abstract A quasi-monolithic second-harmonic-generation ring resonator assembled with miniaturized components is presented. The ring contains a 10-mm-long bulk periodically poled lithium niobate crystal for second-harmonic generation, four plane mirrors and two gradient-index lenses. All parts are mounted on a glass substrate with an overall size of 19.5 mm × 8.5 mm × 4 mm. As pump source a broad-area laser diode operated in an external resonator with Littrow arrangement is utilized. This external cavity diode laser provides near diffraction limited, narrow-bandwidth emission with an optical output power of 450 mW at a wavelength of 976 nm. Locking of the diode laser emission to the resonance frequency of the ring cavity was achieved by an optical self-injection locking technique. With this setup more than 126 mW of diffraction-limited blue light at 488 nm could be generated. The opto–optical conversion efficiency was 28% and a wall plug efficiency better than 5.5% could be achieved.

PACS 140.2020 · 140.3325 · 140.5960 · 190.2620 · 190.4360

D. Skoczowsky (✉) · A. Jechow · R. Menzel
Chair of Photonics, University of Potsdam,
Karl-Liebknecht-Str. 24–25, 14476 Potsdam, Germany
e-mail: danilo.skoczowsky@uni-potsdam.de

H. Stürmer · T. Poßner
Grintech GmbH, Schillerstraße 1, 07745 Jena, Germany

J. Sacher
Sacher Lasertechnik GmbH, Rudolf-Breitscheid-Str. 1–5,
35037 Marburg, Germany

1 Introduction

Compact and highly efficient coherent light sources in the visible spectral region are needed for various applications in spectroscopy, digital printing and medical diagnostics [1, 2]. Especially, wavelengths in the blue and green spectral ranges are of high interest because of the countless number of applications that have been established around the strong emission lines of the argon-ion laser at 488 nm and 514.5 nm. Since those gas lasers are bulky and suffer from low efficiencies and high operation costs they are highly desired to be replaced.

Diode lasers are the most efficient and compact coherent light sources covering a wavelength range from 635 nm to 2600 nm. Because of the broad gain spectrum, diode lasers can be tuned over several nanometers when they are operated in an external cavity. Nowadays, GaN-based devices emitting in the blue spectral range between 365 nm and 475 nm are available. However, between 480 nm and 635 nm no emission from diode lasers is available.

A way to generate laser radiation where no sources are available is nonlinear frequency conversion, i.e. second-harmonic generation (SHG). This field was dominated by the diode pumped solid state lasers (DPSSLs) because high intensities have been necessary to achieve efficient conversion in birefringent phase-matched crystals. The drawback of DPSSLs is that due to the fixed laser transitions of the solid-state materials those devices are restricted to certain wavelengths and their tunability is limited.

Since the introduction of quasi-phase-matched (QPM) materials efficient single-pass frequency conversion with edge-emitting diode lasers has become possible. Several approaches for the generation of visible light with high-brightness laser diodes and QPM materials have been pre-

sented including the use of waveguides [3–8] and bulk nonlinear crystals [9, 10].

Although single-pass SHG stands out by its simplicity and it has the potential to realize miniaturized devices [6], some limitations exist. For efficient single-pass SHG in bulk materials still higher pump powers are demanded. So far, 600 mW of visible cw light has been generated in bulk periodically poled lithium niobate (PPLN) with an opto–optical efficiency of 15% [10]. Higher efficiencies can be achieved with waveguide QPM crystals. However, the laser to waveguide coupling is challenging and the SHG output power is strongly limited by the damage threshold of the material and, furthermore, photorefractive effects can occur. Until now, 160 mW at 488 mW with proton-exchanged PPLN waveguides and 300 mW at 530 nm with PPLN ridge waveguides (RWs) could be demonstrated using distributed feedback (DFB) and distributed bragg reflector (DBR) RW diode lasers, respectively [7, 8].

Higher efficiencies can be realized with resonant SHG. Therefore, the nonlinear crystal is placed inside a high-finesse cavity where the power of the fundamental light is enhanced. Conversion efficiencies of more than 85% have been demonstrated by resonant frequency doubling of cw DPSSLs [11]. By using diode laser master oscillator power amplifiers (MOPAs) to pump resonant SHG, cw output powers of 1 W [12] and efficiencies better than 75% [13] could be achieved in the blue spectral range. Recently, up to 600 mW of blue light could be demonstrated by using a grating-stabilized tapered diode laser and a bowtie ring resonator [14]. A common way to achieve locking between the diode laser frequency and the resonant frequency of the enhancement cavity is to operate the pump laser diode at a fixed injection current and adjust the length of the SH cavity by using piezo mechanics and an electronic loop. This results in rather large setup sizes and very good optical isolation between diode laser and SHG cavity is demanded.

It is also possible to lock diode laser emission to a reference cavity, as demonstrated by Dahmani et al. [15]. This so-called optical self-injection locking was adapted to resonant SHG [16–19]. Sun et al. used feedback from a SHG ring resonator and a grating at the same time [16] to stabilize the diode laser. In another scheme the transmitted light of a linear SHG cavity was fed back to the diode laser via an outer ring resonator [17]. Compact devices could be realized by using monolithic enhancement cavities consisting of crystals with curved and coated facets [18, 19]. In the setup presented by Hemmerich et al. [18], the counterpropagating infrared light was used to provide feedback to the diode laser and maintain locking. However, so far the scheme of optical self locking was only applied to birefringent phase-matched crystals and the achieved SHG output powers have been rather low. In this work we present a quasi-monolithic enhancement ring resonator comprising a 10-mm-long PPLN bulk crystal for efficient SHG at 488 nm. This SHG ring resonator was designed as small as possible with the PPLN crystal being the limiting part. It consists of four mirrors with appropriate reflectivities and two gradient index (GRIN) lenses mounted on a glass substrate to provide high mechanical stability and simple adjustment. A broad-area laser diode (BAL) operated in a V-shaped Littrow external cavity was used as pump laser. This compact external cavity diode laser (ECDL) provides 450 mW of tunable, diffraction-limited and narrow-bandwidth emission at 976 nm. Locking of the diode laser emission to the resonant frequency of the SHG enhancement resonator is realized by the optical self-locking technique utilizing the counterpropagating wave.

2 Experimental setup

2.1 Design and realization of the quasi-monolithic ring resonator

A scheme of the high-finesse ring cavity containing a PPLN crystal is depicted in Fig. 1. The 10-mm-long bulk PPLN bulk crystal was manufactured by HC Photonics. It was made of congruent melt with an MgO doping of 5%. The poling period was 5.36 µm, resulting in QPM for SHG from 976 nm to 488 nm at a temperature of 50°C.

The cavity consisted of four plane mirrors each with a size of 2.5 mm × 2.5 mm × 1 mm. The PPLN crystal was placed between the incoupling mirror R_1 with $R_1 = 0.86$ and the outcoupling mirror R_2 with $R_2 = 0.96$. Furthermore, mirror R_2 is highly reflecting for the blue light which is coupled out via the dichroitic mirror R_3. The fourth mirror R_4 is highly reflecting for the infrared light.

To minimize incoupling losses into the ring cavity the reflectivities of the mirrors R_1 and R_2 have to be impedance matched. Thus, the reflectivity of the mirror R_2 has to com-

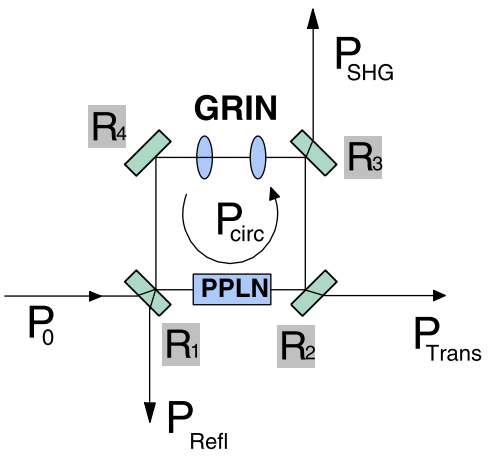

Fig. 1 Schematic drawing of the SHG ring cavity. The reflectivities of the mirrors R_1 and R_2 are impedance matched for the lowest incoupling loss

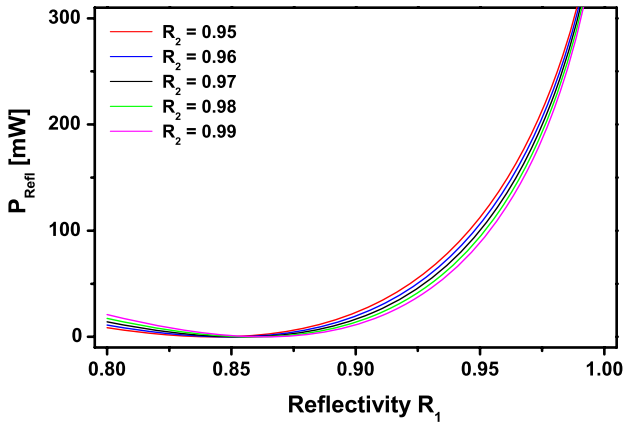

Fig. 2 Calculated reflected power at the incoupling mirror as a function of the reflectivity R_1 for five different outcoupling reflectivities R_2 (assumptions: $P_0 = 450$ mW, $V_0 = 0.03$, $\eta = 3\%/\mathrm{W}$)

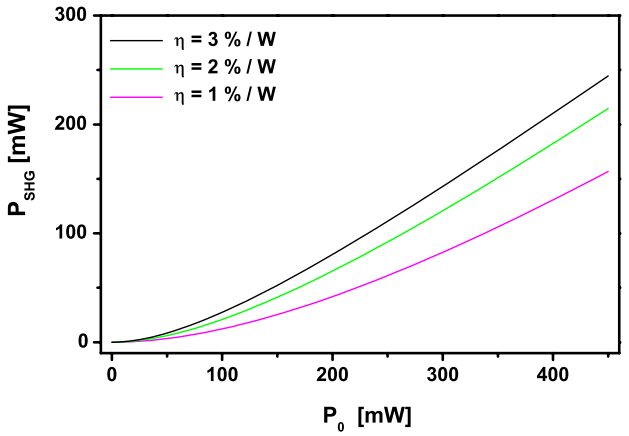

Fig. 3 Calculated power of the generated blue light as a function of the infrared pump power for three different conversion efficiencies of the nonlinear crystal (assumptions: $R_1 = 0.86$, $R_2 = 0.96$, $V_0 = 0.03$)

pensate the sum of all losses inside the resonator. For the reflected power P_{refl} one can derive

$$P_{\mathrm{refl}} = P_0 \left(\frac{\sqrt{R_2}V - \sqrt{R_1}}{1 - \sqrt{R_1 R_2}V} \right)^2. \tag{1}$$

The loss factor V depends on the circulating power P_{circ}. This results from the power-dependent efficiency of the SHG process. Furthermore, the inherent losses inside the ring cavity that originate from non-perfect anti-reflection (AR) coatings or misalignment have to be taken into account. The loss factor then reads

$$V = 1 - V_0 - \eta P_{\mathrm{circ}}, \tag{2}$$

with the cavity loss V_0 and the nonlinear conversion efficiency of the crystal η denoted in W^{-1}. The circulating power is given by the equation

$$P_{\mathrm{circ}} = P_0 \frac{(1 - R_1)R_2}{(1 - \sqrt{R_1 R_2}V)^2}. \tag{3}$$

Figure 2 shows the reflected power as a function of the reflectivity R_1 of the incoupling mirror for five different reflectivities R_2 of the outcoupling mirror.

The power reflected from the ring cavity only slightly depends on the reflectivity of the outcoupling mirror R_2. Also, variations in the loss factor which can result from misalignment do not change the impedance-matching condition significantly. This results from the high efficiency of the nonlinear crystal and the corresponding high losses due to SHG. The optimum reflectivity for the incoupling mirror is $R_1 = 0.86$. For the outcoupling mirror R_2 a moderate reflectivity of 0.96 was chosen to obtain some transmitted light from the ring cavity. This light can be used in further experiments for optical locking of the cavities.

The calculations were done assuming an infrared pump power of $P_0 = 450$ mW, a cavity loss of $V_0 = 0.03$ and an efficiency of the PPLN crystal of $\eta = 0.03\ \mathrm{W}^{-1}$. The power of the generated blue light can be derived using the approximation

$$P_{\mathrm{SHG}} = \eta P_{\mathrm{circ}}^2, \tag{4}$$

which is valid for the described system. The calculated power of the generated blue light for three different conversion efficiencies of the nonlinear crystal are plotted in Fig. 3.

Even when the efficiency of the crystal is reduced the SHG efficiency will remain high. This results from the decreased loss, which leads to a higher circulating power and in turn to a higher conversion of infrared light. Hence, the ring cavity shows self-stabilizing characteristics regarding the SHG efficiency.

The quasi-monolithic ring resonator was assembled on a glass platform with a size of 19.5 mm × 8.5 mm. For easy positioning stop bars for each component have been applied with a diamond-blade saw. The four mirrors have been pre-adjusted with a visible reference laser and were glued onto the platform. Figure 4 shows a picture of the assembled quasi-monolithic ring resonator with the two GRIN lenses and the PPLN bulk crystal.

The GRIN lenses had a length of 3.2 mm and were positioned with a distance of 2.5 mm apart from each other, resulting in an effective focal length of $f = 6.61$ mm. The surface quality of the GRIN lenses was measured to be better than 0.35 (peak to valley) and 0.08 RMS. To minimize the losses inside the cavity the GRIN lenses were AR coated for the pump wavelength. Since the mirrors of the ring cavity were fixed, only the positions of the GRIN lenses could be varied during the experiment. Thus, the distance between the two lenses was adjusted for optimal SHG conversion efficiency. The optical length of the ring cavity is $L = 48.9$ mm, giving a longitudinal mode spacing

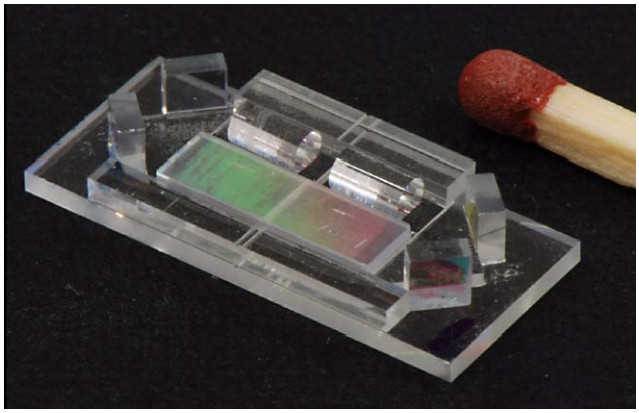

Fig. 4 Quasi-monolithic ring resonator with two GRIN lenses and a PPLN bulk crystal for efficient SHG

of FSR $= c_0/L = 6.1$ GHz with the speed of light in vacuum c_0. The finesse of the ring cavity was calculated to be approximately 20.

2.2 Experimental results

The experimental setup is depicted in Fig. 5. An external cavity diode laser (ECDL) is used to pump resonant SHG using a 10-mm PPLN crystal placed inside the quasi-monolithic ring resonator described earlier. Locking of the diode laser emission to the SHG cavity frequency is maintained by feedback from the counterpropagating infrared light inside the SHG ring resonator back into the ECDL. The feedback power to the BAL amplifier due to the counterpropagating wave was approximately 30 mW.

The ECDL consists of the BAL as gain medium, a fast-axis collimator (FAC), a half-wave plate (HWP) and a diffraction grating with $g = 1800$ mm^{-1}. The gain-guided BAL has an emitter size of $w \times h = 400$ µm $\times$ 1 µm and a cavity length of 1500 µm. To suppress the internal longitudinal and transversal modes of the laser chip the front facet was anti-reflection (AR) coated with a remaining reflectivity of $R < 10^{-4}$. The ECDL is realized in a V-shaped design that was developed to improve the beam quality of a gain-guided BAL [20, 21] and is best understood when separated into the fast-axis and slow-axis parts.

In the direction of the fast axis the BAL possesses a waveguide with a 1-µm aperture and only the fundamental transversal mode will propagate. This highly divergent and diffraction-limited light is collimated with a fast-axis collimator (FAC), an aspherical lens with a high numerical aperture of NA $= 0.8$. The grating is set up to form a Littrow-style resonator in the fast-axis direction with the grating lines positioned parallel to the plane of the slow axis. Thus, wavelength tuning can be realized by tilting the grating in the direction of the fast axis and changing the Littrow angle, respectively. Since the laser diode emission is TE polarized, a half-wave plate is necessary to rotate the electric field by 90°. In this direction longitudinal mode selection is realized, while the transversal mode remains unaffected.

In the direction of the slow axis the BAL diode is substructured as a stripe array by gain guiding. Contact stripes with a pitch of $d = 10$ µm and a width of 3 µm are applied onto the active region. Thus, pumped and unpumped regions alternate and beneath each contact stripe a transversal fundamental mode will propagate. An anti-phase oscillation between the emissions of neighboring stripes was observed resulting in a far-field pattern with a double lobe. The angle of the two lobes follows a simple interference pattern $\sin\alpha = \pm\lambda/2d$. With the pitch of the contact stripes of $d = 10$ µm and the wavelength $\lambda = 976$ nm a feedback angle of $\alpha = \pm 48.8$ mrad can be calculated. By applying feedback

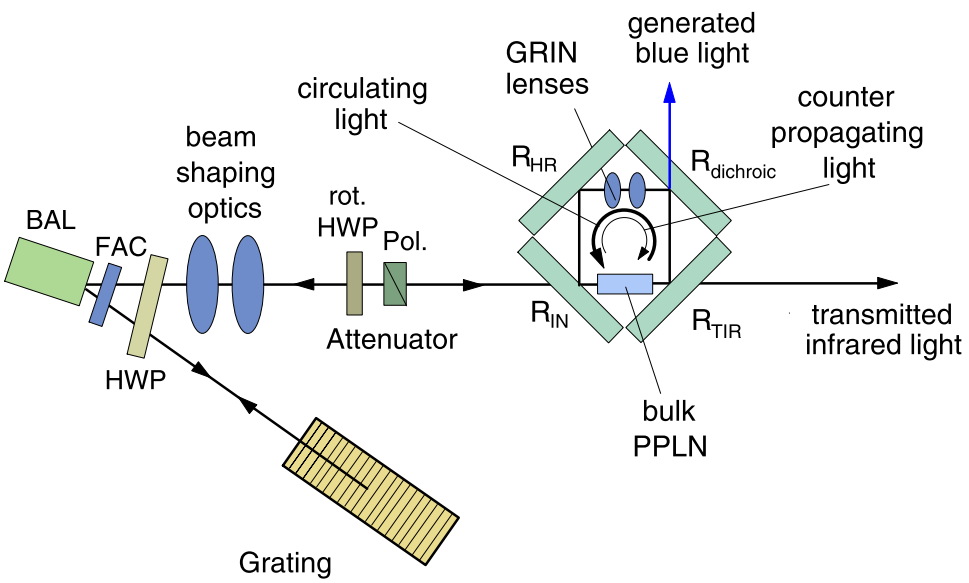

Fig. 5 Sketch of the experimental setup in the plane of the slow axis of the broad-area laser. The light of a frequency-stabilized broad-area laser diode (BAL) is coupled via a beam-shaping optics and an attenuator into a miniaturized ring resonator containing a PPLN crystal for SHG and two GRIN lenses

to the laser diode under this specific angle α, the anti-phase oscillation is enforced [20]. This leads to constructive interference of the fundamental modes that arise beneath each contact stripe and a nearly diffraction limited output under the angle $-\alpha$ will be achieved. Because the grating acts similar to a plane mirror in the direction of the slow axis, the feedback angle α can be selected by tilting the grating.

The astigmatism of the ECDL emission was corrected by the use of three cylindrical lenses. Two lenses in the slow-axis direction ($f = 300$ mm and $f = 60$ mm) and one lens in the fast-axis direction ($f = 40$ mm) were used to create a focus with a symmetric beam waist radius of $w_0 = 16$ µm in both axes.

Inside the ring cavity only the fundamental transversal mode can propagate while all other modes will experience losses. Furthermore, the high Q of the ring will only allow narrow-bandwidth light to circulate. Thus, the SHG ring cavity can be understood as a transversal and longitudinal mode filter. The ECDL emission is locked onto the SHG cavity by the feedback of the counterpropagating infrared light. The counterpropagating field arises from partial surface reflections due to non-perfect AR coatings of the optical elements inside the ring resonator and is sufficient to seed the BAL amplifier onto the desired frequency. This self-injection locking mechanism results in a passive coupling of both cavities. A similar technique was used in combination with a monolithic ring resonator [19]. A discussion about other types of optical self-injection locking is provided in [22].

The ECDL was operated at a fixed injection current of 1.8 A with a corresponding output power of 450 mW. At this operating condition the beam propagation factors in both axes were measured to be better than $M^2 < 1.2$. A spectral line width below 1 GHz was determined. Furthermore, the light was tunable over more than 30 nm with a center wavelength of 970 nm. Figure 6 shows the blue output power as a function of the circulating infrared power inside the ring cavity. The crystal was temperature stabilized at 30°C. The output power of the infrared light and, thus, the circulating power was varied using an attenuator.

With an infrared laser output power of 450 mW, a maximum blue output power of 126.7 mW was achieved. At this operating point the transmitted infrared output power was measured to be 80 mW and, with the known reflectivity of the outcoupling mirror, a circulating power of $P_{\mathrm{circ}} = 2.0$ W results. The normalized conversion efficiency of the PPLN crystal was calculated to be $\eta = 3.1\%/\mathrm{W}$. This is only slightly lower than the value obtained with the single-pass setup.

The beam propagation factors were measured with the moving slit technique (modified Beam scope P5, Data Ray Inc.). The beam waist radii were determined using the second-order moments of the intensity distribution. The M^2 values were calculated from a hyperbolic fit through the data. This follows completely the ISO11146 standard [23]. The caustic of the generated blue light at a laser diode injection current of 1.8 A and a blue output power of 120 mW is depicted in Fig. 7. Beam propagation factors of $M^2_{\mathrm{fast}} < 1.05$ for the fast axis and $M^2_{\mathrm{slow}} < 1.1$ for the slow axis have been obtained.

Figure 8 shows the spectrum of the generated blue light measured with an optical spectrum analyzer (OSA–Ando AQ-A6315A) at a maximum output power of 120 mW. At a crystal temperature near room temperature (30°C) a center wavelength of 487.5 nm was determined. The width of the spectrum (FWHM) was measured to be 50 pm, which is the resolution limit of the OSA. The side mode suppression ratio was better than 40 dB.

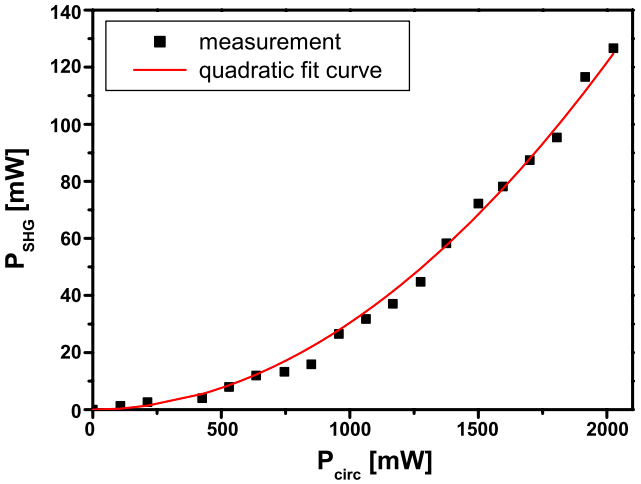

Fig. 6 Output power of the generated blue light as a function of the incident infrared power with quadratic fit curve

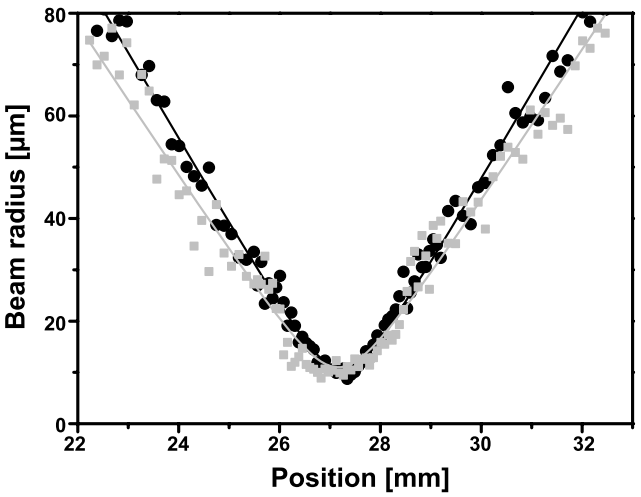

Fig. 7 Caustic of the generated blue light at an optical output power of 120 mW. The beam quality was determined to be better than $M^2 < 1.1$ for both axes

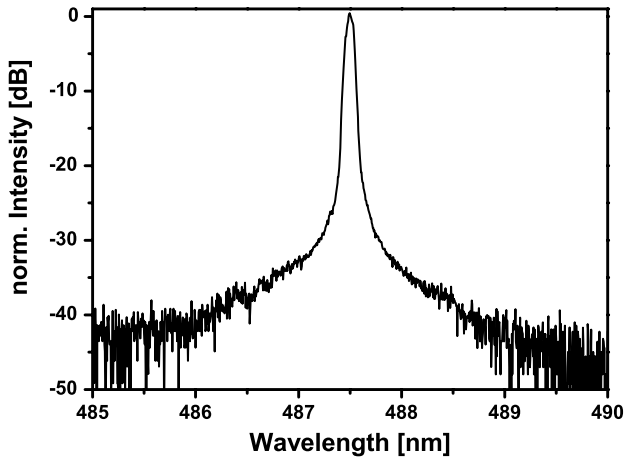

Fig. 8 Spectrum of the generated blue light at an injection current of 1.8 A and a PPLN temperature of 30°C

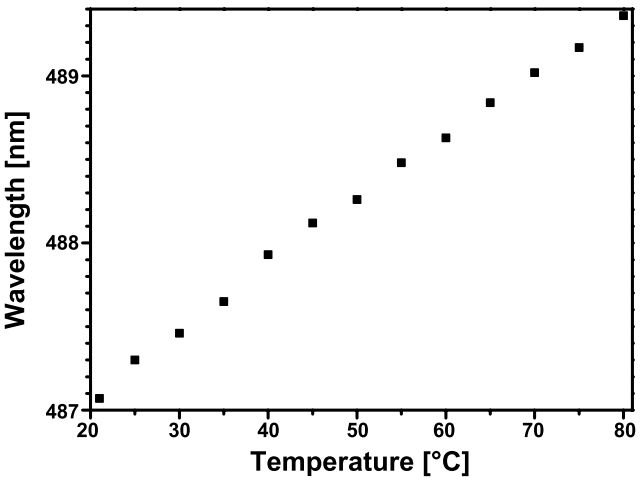

Fig. 9 Center wavelength of the blue light as a function of the PPLN crystal temperature. A tuning range of more than 2 nm was achieved

By changing the crystal temperature it was possible to tune the emission wavelength of the blue light. Therefore, the wavelength of the ECDL emission had to be adjusted to achieve the state of self locking. This was done by tilting the grating and changing the Littrow angle, respectively. A continuous tuning is not possible because of the longitudinal mode spacing inside the ring cavity.

By changing the crystal temperature from room temperature to about 80°C, a tuning range of more than 2 nm with a temperature coefficient of $\alpha = 0.038$ nm/K was achieved as depicted in Fig. 9. The optical output powers were well above 100 mW for all cases.

3 Conclusion

A new compact ring resonator assembled with miniaturized components is presented. A quasi-monolithic setup was realized with four plane mirrors glued onto a glass platform with a size of 19.5 mm × 8.5 mm. The ring cavity contained a 10-mm-long bulk PPLN crystal to achieve efficient SHG of diode laser emission. Two GRIN lenses were used to maintain resonator round-trip stability.

An ECDL system containing a stripe array BAL as gain medium was used to pump SHG inside this resonator. The locking of the ECDL emission to the ring resonator modes was achieved by a weak back reflection of the counterpropagating infrared light inside the SHG cavity. No electronic loop or piezo actuators have been used for the locking of the two cavities.

With this setup it was feasible to generate an optical output power of more than 125 mW of diffraction-limited laser emission at a wavelength of 488 nm.

The opto–optical conversion efficiency from the infrared to the visible was better than 28% with a resulting wall plug efficiency of 5.5%. This high conversion efficiency was possible because the infrared emission of the ECDL was enhanced by a factor of 4.5 inside the ring cavity. The beam propagation factors of the blue light were measured to be better than $M^2 < 1.1$ in both axes. The generated blue light showed almost no astigmatism or ellipticity.

To our knowledge, this is the first demonstration of a compact quasi-monolithic enhancement resonator containing a quasi-phase-matched crystal. Furthermore, the achieved opto–optical conversion efficiency of 28% represents the highest value obtained with a single broad-area laser diode and SHG.

Acknowledgements The authors thank Volker Raab from Optikexpertisen for helpful discussion. This work was funded by the Pro Inno II project 'Blue ring resonator' of the Federal Ministry of Economics and Technology (BMWi) and the German Federation of Industrial Research Associations (AiF).

References

1. T. Vo-Dinh, B. Cullum, P. Kasili, J. Phys. D: Appl. Phys. **36**, 1663 (2003)
2. D. Lenz, A.O. Gerstner, W. Laffers, M. Steinbrecher, F. Bootz, A. Tarnok, Proc. SPIE **4962**, 364 (2003)
3. R.G. Batchko, M.M. Fejer, R.L. Byer, D. Woll, R. Wallenstein, V.Y. Shur, L. Erman, Opt. Lett. **24**, 1293 (1999)
4. T. Sugita, K. Mizuuchi, Y. Kitaoka, K. Yamamoto, Opt. Lett. **24**, 1590 (1999)
5. Z. Ye, Q. Lou, J. Dong, Y. Wei, L. Lin, Opt. Lett. **30**, 73 (2005)
6. M. Maiwald, D. Jedrzejczyk, A. Sahm, K. Paschke, R. Güther, B. Sumpf, G. Erbert, G. Tränkle, Opt. Lett. **34**, 217 (2009)
7. A. Jechow, M. Schedel, S. Stry, J. Sacher, R. Menzel, Opt. Lett. **32**, 3035 (2007)
8. H.K. Nguyen, M.H. Hu, Y. Li, K. Song, N.J. Visovsky, S. Coleman, C.-E. Zah, Proc. SPIE **6890**, 68900I (2008)
9. A. Jechow, R. Menzel, Appl. Phys. B **89**, 507 (2007)
10. M. Maiwald, S. Schwertfeger, R. Güther, B. Sumpf, K. Paschke, C. Dzionk, G. Erbert, G. Tränkle, Opt. Lett. **31**, 802 (2006)
11. Z.Y. Ou, S.F. Pereira, E.S. Polzik, H.J. Kimble, Opt. Lett. **17**, 640 (1992)

12. D. Woll, B. Beier, K. Boller, R. Wallenstein, M. Hagberg, S. O'Brien, Opt. Lett. **24**, 691 (1999)
13. R. Le Targat, J.-J. Zondy, P. Lemonde, Opt. Commun. **247**, 471 (2005)
14. J.H. Lundeman, O.B. Jensen, P.E. Andersen, S. Andersson-Engels, B. Sumpf, G. Erbert, P.M. Petersen, Opt. Express **16**, 2486 (2008)
15. B. Dahmani, L. Hollberg, R. Drullinger, Opt. Lett. **12**, 876 (1987)
16. X.G. Sun, G.W. Switzer, J.L. Carlsten, Appl. Phys. Lett. **76**, 955 (2000)
17. G.J. Dixon, C.E. Tanner, C.E. Wieman, Opt. Lett. **14**, 731 (1989)
18. A. Hemmerich, C. Zimmermann, T.W. Hänsch, Appl. Opt. **33**, 988 (1994)
19. W.J. Kozlovsky, W.P. Risk, W. Lenth, B.G. Kim, G.L. Bona, H. Jaeckel, D.J. Webb, Appl. Phys. Lett. **65**, 525 (1994)
20. W.P. Risk, T.R. Gosnell, A.V. Nurmikko, *Compact Blue–Green Lasers* (Cambridge University Press, Cambridge, 2003)
21. V. Raab, R. Menzel, Opt. Lett. **27**, 167 (2002)
22. A. Jechow, V. Raab, R. Menzel, M. Cenkier, S. Stry, J. Sacher, Opt. Commun. **277**, 161 (2007)
23. International Organization for Standardization, *Lasers and Laser-related Equipment—Test Methods for Laser Beam Parameters—Beam Widths, Divergence Angle and Beam Propagation Factor* (ISO 11146, Geneva, 2004)